SAGE-Hindawi Access to Research
Enzyme Research
Volume 2011, Article ID 294724, 7 pages
doi:10.4061/2011/294724

Research Article

Inhibitory Effect of Phthalic Acid on Tyrosinase: The Mixed-Type Inhibition and Docking Simulations

Shang-Jun Yin, Yue-Xiu Si, and Guo-Ying Qian

College of Biological and Environmental Sciences, Zhejiang Wanli University, Ningbo 315100, China

Correspondence should be addressed to Shang-Jun Yin, yinshangjun@163.com and
Guo-Ying Qian, qianguoying_wanli@hotmail.com

Received 17 March 2011; Accepted 23 March 2011

Academic Editor: Yong-Doo Park

Tyrosinase inhibition studies are needed due to the medicinal applications such as hyperpigmentation. For probing effective inhibitors of tyrosinase, a combination of computational prediction and enzymatic assay via kinetics was important. We predicted the 3D structure of tyrosinase, used a docking algorithm to simulate binding between tyrosinase and phthalic acid (PA), and studied the reversible inhibition of tyrosinase by PA. PA inhibited tyrosinase in a mixed-type manner with a $K_i = 65.84 \pm 1.10$ mM. Measurements of intrinsic and ANS-binding fluorescences showed that PA induced changes in the active site structure via indirect binding. Simulation was successful (binding energies for Dock6.3 $= -27.22$ and AutoDock4.2 $= -0.97$ kcal/mol), suggesting that PA interacts with LEU73 residue that is predicted commonly by both programs. The present study suggested that the strategy of predicting tyrosinase inhibition based on hydroxyl groups and orientation may prove useful for screening of potential tyrosinase inhibitors.

1. Introduction

Melanogenesis is a complex mechanism for melanin pigment production. Tyrosinase (monophenol, dihydroxyphenylalanine: oxygen oxidoreductase, EC 1.14.18.1) plays a central role in melanin synthesis as a copper-binding metalloenzyme. It is ubiquitously distributed in organisms and has multi catalytic functions such as the hydroxylation of tyrosine to DOPA, the oxidation of DOPA to DOPAquinone, and the oxidation of 5,6-dihydroxyindole [1–3]. Besides the catalytic features, tyrosinase is distinctive from the other enzymes as it displays various inhibition patterns. Several previous studies suggest [4–6] that tyrosinase can induce neurotoxicity by activating apoptotic stress signaling pathways and is directly associated with a neurotoxic overproduction of cellular dopamine. It implies that tyrosinase gene expression results in oxidative metabolites and reactive oxygen species at the cellular level which are known to have cytotoxic effects.

Tyrosinase is directly related with severe skin diseases such as type 1 albinism (http://albinismdb.med.umn.edu/) and melanoma [7–9]. Mutations of tyrosinase gene can cause severe skin disease such as oculocutaneous albinism (OCA). Three types of OCA—tyrosinase-negative, yellow-mutant, and temperature-sensitive OCA—have been well known [10, 11], and new subtypes of albinism have been reported [12]. Tyrosinase is also involved in the skin hyperpigmentation and in this regard, tyrosinase inhibition study is directly associated with the treatment of melanin overproduction [13–15].

The tyrosinase mechanism is complex, in that this enzyme can catalyze multiple reactions. The crystallographic structure of tyrosinase has not been determined; thus, the overall 3D structure and architecture of the active site are not well understood regardless of several reports [16–18]. Studies of this enzyme mechanism must involve a variety of computational methods and kinetics to derive the structure-function relationships, for example, between substrates and ligands of the enzyme.

In the current study we determined the mechanism of tyrosinase inhibition by PA using computational simulation and kinetic analysis. We hypothesized that the two hydroxyl groups of PA may block L-DOPA oxidation by binding to tyrosinase. Previous findings have shown the importance of

hydroxyl groups in tyrosinase inhibition [19–22] in terms of molecular position, number, and specific interactions with the enzyme; these findings further support our hypothesis. PA has two hydroxyl groups, thus implying that PA might have an inhibitory effect on tyrosinase. Direct use of PA in medicinal or cosmetic applications is limited due to the toxicity; however, effective approaches derived from the combination of computational simulation and enzymatic kinetics as an example case are of interest for further screening tyrosinase inhibitor candidates. The computational simulation suggested that PA could be a potent inhibitor for tyrosinase where PA can directly interact with some residues locating near to the active site. Experimentally, PA exerts a mixed type of inhibition on tyrosinase. Kinetic parameters have consistently supported the result of docking simulation, and measurements of ANS-binding fluorescence have revealed changes in the regional structure. A combination of inhibition kinetics and computational modeling may facilitate testing of potential tyrosinase inhibitors, such as PA and prediction of the inhibitory mechanisms.

2. Materials and Methods

2.1. Materials. Tyrosinase (M.W. 128 kDa), L-DOPA, and PA were purchased from Sigma-Aldrich (Seoul, Korea). When L-DOPA was used as a substrate in our experiments, the purchased tyrosinase had a K_m of 0.30 ± 0.02 mM ($V_{\max} = 0.13 \pm 0.05$ mmol·min^{-1}) according to a Lineweaver-Burk plot. All kinetic reactions and measurements in this study were performed in 50 mM sodium phosphate buffer (pH 6.9).

2.2. Tyrosinase Assay and Kinetic Analysis for the Mixed-Type Inhibition. A spectrophotometric tyrosinase assay was performed as previously described [23, 24]. To begin the assay, a 10-μL sample of enzyme solution was added to 1 mL of reaction mix. Tyrosinase activity (v) was recorded as the change in absorbance per min at 492 nm using a Perkin Elmer Lambda Bio U/V spectrophotometer. To describe the mixed-type inhibition mechanism, the Lineweaver-Burk equation in double reciprocal form can be written as

$$\frac{1}{v} = \frac{K_m}{V_{\max}}\left(1 + \frac{[\mathrm{I}]}{K_i}\right)\frac{1}{[\mathrm{S}]} + \frac{1}{V_{\max}}\left(1 + \frac{[\mathrm{I}]}{\alpha K_i}\right). \quad (1)$$

Secondary plots can be constructed from

$$\text{Slope} = \frac{K_m}{V_{\max}} + \frac{K_m[\mathrm{I}]}{V_{\max}K_i}, \quad (2)$$

$$Y\text{-intercept} = \frac{1}{V_{\max}^{\mathrm{app}}} = \frac{1}{V_{\max}} + \frac{1}{\alpha K_i V_{\max}}[\mathrm{I}]. \quad (3)$$

Then, the α, K_i, K_m, and $V_{\max}$ values can be derived from the above equations. The secondary replot of Slope or Y-intercept versus [I] is linearly fitted, assuming a single inhibition site or a single class of inhibition site, as shown in Scheme 1.

2.3. Intrinsic and ANS-Binding Fluorescence Measurements. Fluorescence emission spectra were measured with a Jasco FP750 spectrofluorometer using a cuvette with a 1-cm path length. Tryptophan fluorescence was measured following excitation at 280 nm, and the emission wavelength ranged between 300 and 410 nm. Changes in the ANS-binding fluorescence of tyrosinase were measured following excitation at 390 nm, and the emission wavelength ranged from 400 to 520 nm. The tyrosinase was labeled with 40 μM ANS for 30 min prior to measurements.

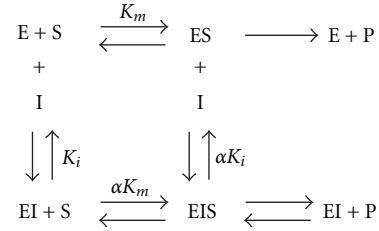

Scheme 1

2.4. Determination of the Binding Constant and the Number of Binding Sites. According to a previous report [25], when small molecules are bound to equivalent sites on a macromolecule, the equilibrium between free and bound molecules is given by the following equation:

$$\frac{F_0}{F_0 - F} = \frac{1}{n} + \frac{1}{K}\frac{1}{[Q]}, \quad (4)$$

where F_0 and F are the relative steady-state fluorescence intensities in the absence and presence of quencher, respectively, and [Q] is the quencher (PA) concentration. The values for the binding constant (K) and number of binding sites (n) can be derived from the intercept and slope of a plot based on (4).

2.5. Homology Modeling of Tyrosinase and Docking Simulations. The 3D structure of tyrosinase from *Agaricus bisporus* was modeled using the SWISS-MODEL [26] to assemble 556 amino acids (Protein CAA11562) selected with a homology-modeling protocol. This method differs from those described in previous reports [17, 18]. We retrieved the known homologues of tyrosinase (average, 23% sequence identity), as well as partial tyrosinase homologues, from the Protein Data Bank (PDB) (http://www.pdb.org/) and identified a PDB entry (2zmx chain A) to provide a suitable structural template. Based on the sequence alignment, the 3D structure of tyrosinase was constructed with a high level of confidence (final total energy, 38297.020 KJ/mol).

Among the many tools available for protein-ligand docking, Dock6.3 and Autodock4.2 programs were applied because of their automated capability [27]. The program uses a set of predefined 3D grids of the target protein with a systematic search technique [28]. The original structure of PA was derived from the PubChem database (Compound ID: 1017, http://pubchem.ncbi.nlm.nih.gov/). To prepare for the docking procedure, the following steps were taken: (1) conversion of 2D structures to 3D structures; (2)

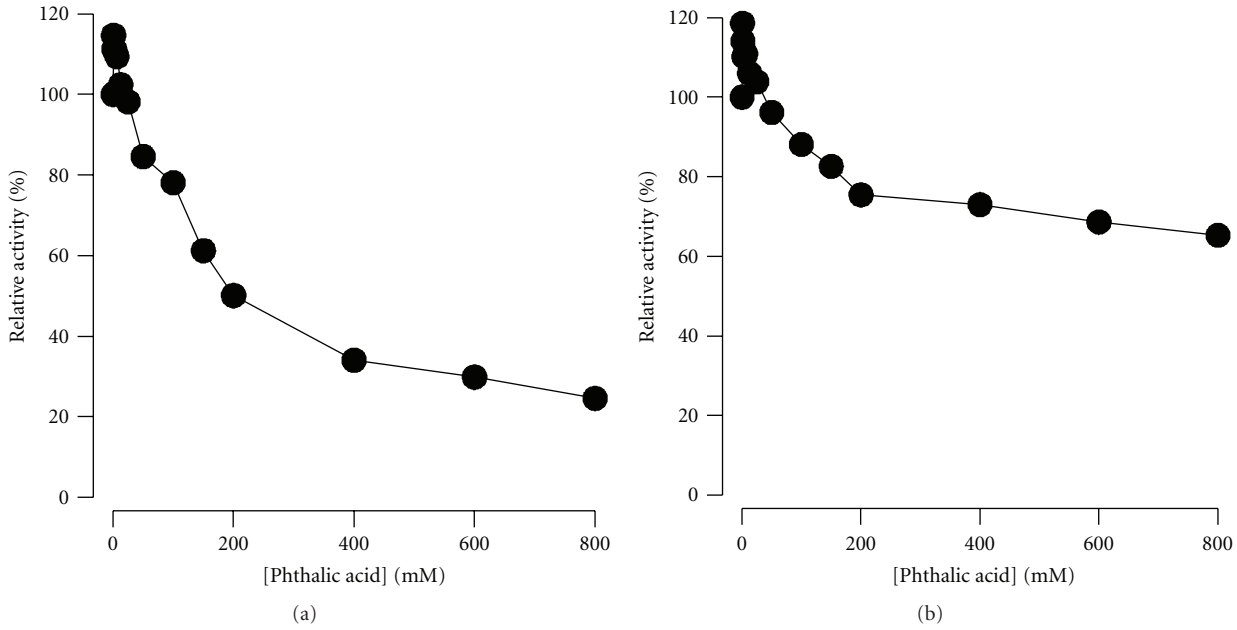

Figure 1: Inhibitory effect of PA on tyrosinase. Data are presented as the means ($n = 3$). Tyrosinase was incubated with PA at various concentrations for 3 h at 25°C and then added to the assay system at the corresponding PA concentrations (a) or in the absence of PA. (b) The final concentrations of L-DOPA and tyrosinase were 2 mM and 2.0 μg/mL, respectively.

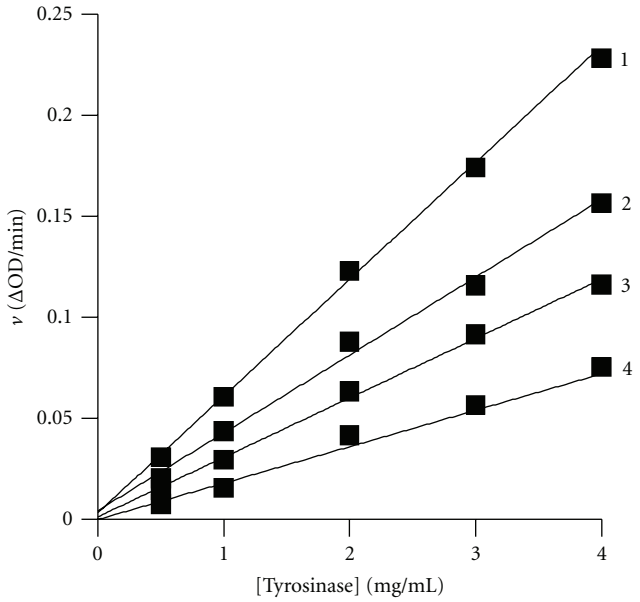

Figure 2: Plots of v versus [E]. The v value indicates the change in absorbance at 492 nm per minute at PA concentrations of 0, 100, 200, and 400 mM (labels 1 to 4, resp.). The final L-DOPA concentration was 2 mM.

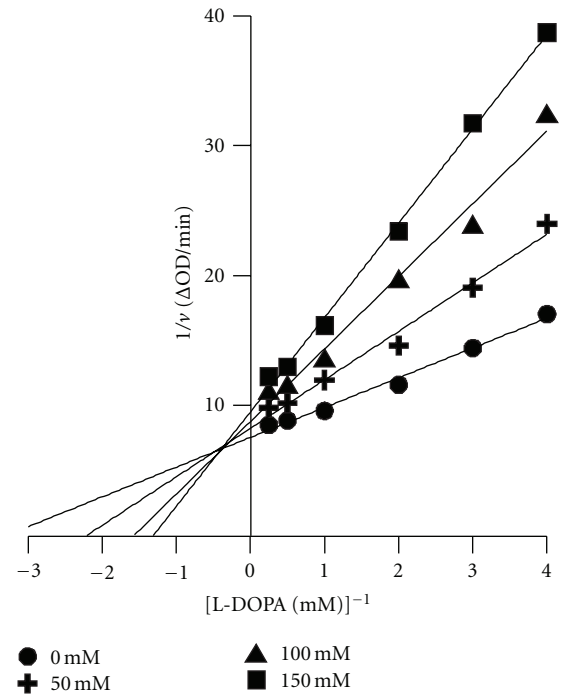

Figure 3: Lineweaver-Burk plot. (a) The PA concentrations were 0 (•), 50 (+), 100 (▲), and 150 mM (■). (b) The final enzyme concentration was 2.0 μg/mL.

calculation of charges; (3) addition of hydrogen atoms; (4) location of pockets. For these steps, we used OpenEye (http://www.eyesopen.com/).

3. Results

3.1. Effect of PA on Tyrosinase Activity. We assayed tyrosinase activity changes in the presence of PA. Tyrosinase activity was conspicuously inactivated by PA in a dose-dependent manner with an IC_{50} of 200 ± 5.0 mM ($n = 3$), where PA was present both in reaction and assay buffers (Figure 1(a)). At less than 50 mM PA, tyrosinase was slightly activated up to 18% and, then, gradually inactivated by increasing PA concentration (Figure 1(a)). When PA was removed from

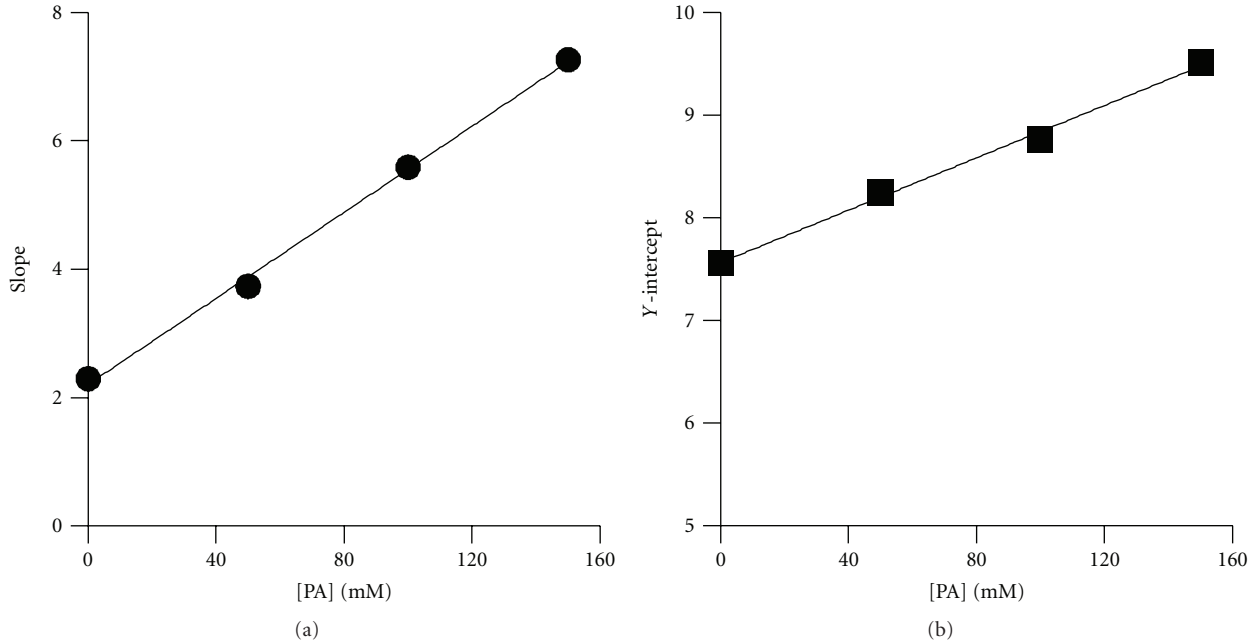

Figure 4: Secondary replots. (a) Plot of Slope versus [PA]. All data were collected from Lineweaver-Burk plots. The replot was plotted based on (2). (b) Plot of Y-intercept versus [PA]. The replot was plotted based on (3).

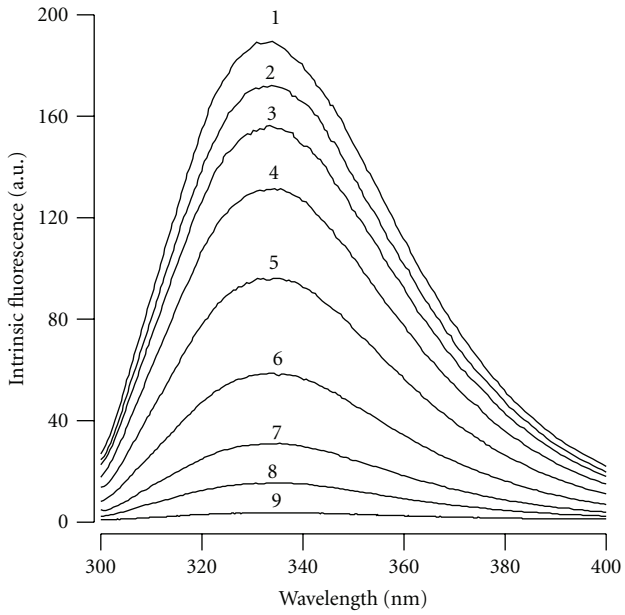

Figure 5: Intrinsic fluorescence changes by PA. Tyrosinase was incubated with PA for 3 h before measurements. Label 1 represents the native state. Labels 2 through 9 indicate PA concentrations of 1.56, 3.125, 6.25, 12.5, 25, 50, 100, and 400 mM, respectively.

the assay buffer, the residual activity was higher than 60% even at 800 mM PA ($n = 3$), implying that PA reversibly binds to tyrosinase (Figure 1(b)). The phenomenon of slight activation by PA at the low concentration was also observed in Figure 1(b).

To confirm the reversibility of PA-mediated inhibition, plots of the remaining activity versus [E] were constructed (Figure 2). The results showed straight lines passing through the origin, indicating the PA-mediated reversible inhibition, as predicted in results of Figure 1.

3.2. Lineweaver-Burk Plot Analysis of Tyrosinase Inhibition by PA. We adapted Lineweaver-Burk plot analysis to elucidate inhibition type and mechanism of PA on tyrosinase. The results showed changes in both the apparent $V_{\max}$ and the K_m, indicating that PA induced a mixed type of inhibition (Figure 3). The secondary replots of Slope versus (PA) and Y-intercept versus (PA) were linearly fitted (Figures 4(a) and 4(b)), showing that PA has a single inhibition site or a single class of inhibition site on tyrosinase. Using (1)–(3), the α-value was calculated to be 9.05 ± 1.4 ($n = 2$), and the K_i was 65.84 ± 1.10 mM ($n = 2$).

3.3. Effect of PA on Tyrosinase Tertiary Structure Spectrofluorimetry Studies. Next, we measured the intrinsic fluorescence changes of tyrosinase in the presence of PA. We found that the intrinsic fluorescence of tyrosinase is changed significantly accompanying a quenching effect, which gradually decreased with no significant shift of the maximum peak wavelength (Figure 5). At 400 mM, PA completely quenched the fluorescence. For calculating binding affinity, a double reciprocal plot was evaluated according to (4) as shown in Figure 6. The result revealed a linear relationship, we calculated the binding constant to be $K = 0.068 \pm 0.03\ \text{mM}^{-1}$, and the binding number was $n = 1.01 \pm 0.65$ by using (4).

To compare the intrinsic fluorescence result and further to elucidate the changes in tyrosinase hydrophobicity due to alterations of the active site shape by PA, the ANS-binding fluorescence changes were monitored in the presence

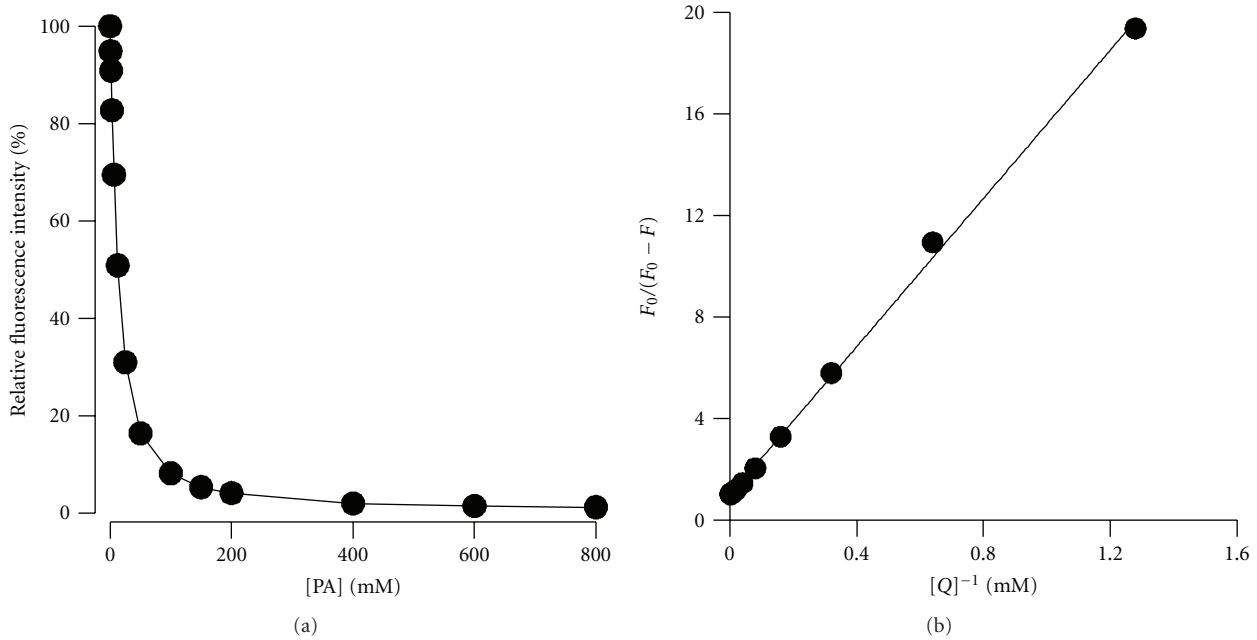

Figure 6: Plot of maximum fluorescence intensity versus [PA]. (a) Tyrosinase was incubated with various concentrations of PA (1.56 to 800 mM). (b) Double reciprocal plot of $F_0/(F_0 - F)$ versus $[Q]^{-1}$. Data was treated according to (4). F_0 maximum native fluorescence intensity; F maximum fluorescence intensity of sample; Q quencher PA.

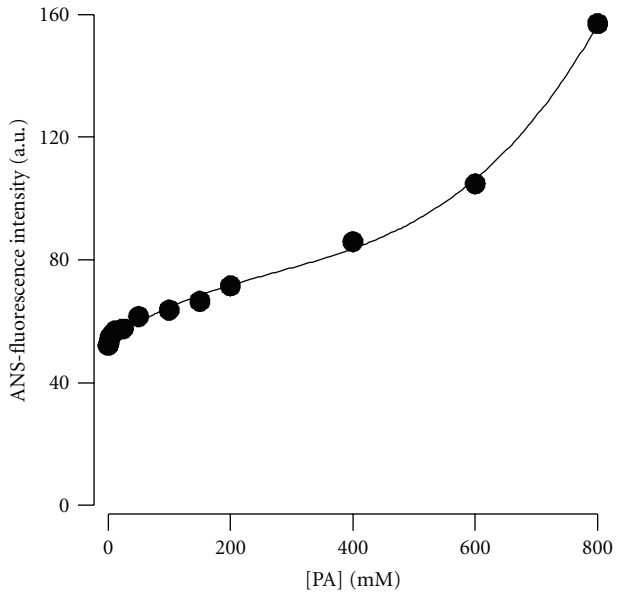

Figure 7: Changes in ANS-binding fluorescence of tyrosinase at different PA concentrations. ANS (40 μM) was incubated with tyrosinase for 30 min to label the hydrophobic enzyme surfaces prior to fluorescence measurements. Data are presented as the means ($n = 2$).

of PA (Figure 7). PA gradually increased the ANS-binding fluorescence of tyrosinase in a dose-dependent manner, an indication that binding to inhibitor exposed the hydrophobic surfaces within the tyrosinase, which might be mainly caused from the active site.

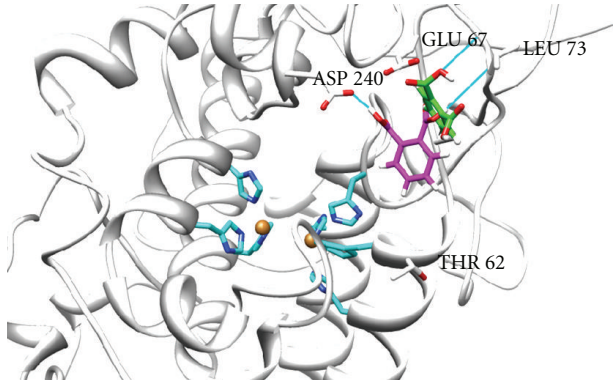

Figure 8: Computational docking simulation of binding between tyrosinase and PA. The modeled 3D structure of tyrosinase using SWISS-MODEL to assemble 556 amino acids selected with a homology-modeling protocol. Two copper ions (balls) coordinated with six histidines, as indicated the blue colors in the figure. The pink stick is PA as docked by Dock6.3. The green stick is PA as docked by AutoDock4.2.

3.4. Computational Prediction of 3D Tyrosinase Structure and Docking Simulation of PA Binding. Because the crystallographic structure of tyrosinase is not available, we selected a template structure from the PDB (2zmxA) to simulate the 3D structure of tyrosinase. In the predicted structure of tyrosinase, a binding pocket is indicated with two coppers: one is coordinated to HIS38, HIS54, and HIS63, and the other is coordinated to HIS190, HIS194, and HIS216, respectively (Figure 8). The docking simulation of binding between PA and tyrosinase was successful in producing a significant

score (binding energy for Dock6.3 was −27.22 kcal/mol). We searched for PA-binding residues within tyrosinase that were close to each other and found the most important residues at THR62, GLU67, LEU73, and ASP240 predicted from Dock6.3. In the same way, AutoDock4.2 was also applied to probe docking sites. As a result, PA-binding residues were predicted as GLU67 and LEU73 with a relatively low score (binding energy for AutoDock4.2 was −0.97 kcal/mol). We found that LEU73 has been commonly predicted from both programs. The docking simulations provided informative data for the PA as a tyrosinase inhibitor by identifying binding residues near to active site pocket, which might directly affect the L-DOPA substrate docking and catalysis by inducing regional structure changes.

4. Discussion

Previous studies have recognized an apparently potent inhibitory effect of compounds with hydroxyl groups on tyrosinase [29–32]. In this context, we hypothesized that PA could be a potent tyrosinase inhibitor due to the structural aspect with two hydroxyl groups. To confirm our supposition, we simulated the docking between PA and tyrosinase and conducted kinetic studies. As a result, we found that PA was directly involved with tyrosinase inhibition not via copper chelation but via mixed-type manner. Experimentally, our kinetic studies consistently confirmed all results and the model described in Scheme 1. The inhibitory mechanism of PA was partly similar to those of copper chelators but still has different aspect that PA did not directly bind to coppers at the active site [33, 34]. V_{max} value changes were predicted by docking simulation that PA might not compete with L-DOPA for docking because the binding sites are not located in the active site pocket. However, the K_m changes occurred in more complex manner: L-DOPA did not directly compete with PA but the L-DOPA accessibility for docking to coppers at the active site could be affected by the PA-docking-induced conformational changes resulting in the tertiary shape of active site, and this conformational change was confirmed by monitoring the hydrophobic surface changes of tyrosinase. This is due to the reason that PA docking site is very near to the active site where L-DOPA oxidation is occurred. Thus, the mixed-type inhibition of tyrosinase by PA was observed.

Using computational simulations, we predicted that PA bound directly with several residues (among them LEU73 is the most significant) of tyrosinase. This result is consistently matched to the data in Figure 6 where the number of binding site is calculated as approximately one. LEU73 residue is thought to be involved in the first stage of PA binding. Because the PA binding site is quite different to the L-DOPA binding site, it is not overlapped, but relatively in close proximity, which may allow PA binding to interact with the enzyme-substrate intermediate or another step in catalysis (V_{max} changes), and inducing detectable hydrophobic changes in the active site may result in retarding L-DOPA accession (K_m changes). Overall, the experimental data fit very well with data predicted by the simulations.

Taken together, our study provides new insight into the role of several residues in tyrosinase and provides useful information regarding the 3D structure of tyrosinase. A combination of inhibition kinetics and computational modeling may facilitate the testing of potential tyrosinase inhibitors and the prediction of their inhibitory mechanisms. The present study also suggested that the strategy of predicting tyrosinase inhibition based on hydroxyl groups and orientation may prove useful for the screening of potential tyrosinase inhibitors.

Abbreviations

DOPA: 3,4-dihydroxyphenylalanine
PA: Phthalic acid
ANS: 1-anilinonaphthalene-8-sulfonate.

Acknowledgments

This paper was supported by grants of Key Science and Technology Innovation Teams of Zhejiang Province (Grants no. 2009R50031 and no. 2009R50031-1) from the Science and Technology Department of Zhejiang Province and the Zhejiang Provincial Top Key Discipline of Modern Microbiology and Application (Grants no. KF2010006 and no. KF2010007).

References

[1] C. Olivares and F. Solano, "New insights into the active site structure and catalytic mechanism of tyrosinase and its related proteins," *Pigment Cell and Melanoma Research*, vol. 22, no. 6, pp. 750–760, 2009.

[2] F. García-Molina, J. L. Muñoz, R. Varón, J. N. Rodríguez-López, F. García-Cánovas, and J. Tudela, "A review on spectrophotometric methods for measuring the monophenolase and diphenolase activities of tyrosinase," *Journal of Agricultural and Food Chemistry*, vol. 55, no. 24, pp. 9739–9749, 2007.

[3] K. Jimbow, J. S. Park, F. Kato et al., "Assembly, target-signaling and intracellular transport of tyrosinase gene family proteins in the initial stage of melanosome biogenesis," *Pigment Cell Research*, vol. 13, no. 4, pp. 222–229, 2000.

[4] T. Hasegawa, A. Treis, N. Patenge, F. C. Fiesel, W. Springer, and P. J. Kahle, "Parkin protects against tyrosinase-mediated dopamine neurotoxicity by suppressing stress-activated protein kinase pathways," *Journal of Neurochemistry*, vol. 105, no. 5, pp. 1700–1715, 2008.

[5] R. E. Boissy and P. Manga, "On the etiology of contact/occupational vitiligo," *Pigment Cell Research*, vol. 17, no. 3, pp. 208–214, 2004.

[6] E. Nishioka, Y. Funasaka, H. Kondoh, A. K. Chakraborty, Y. Mishima, and M. Ichihashi, "Expression of tyrosinase, TRP-1 and TRP-2 in ultraviolet-irradiated human melanomas and melanocytes: TRP-2 protects melanoma cells from ultraviolet B induced apoptosis," *Melanoma Research*, vol. 9, no. 5, pp. 433–443, 1999.

[7] T. G. Salopek and K. Jimbow, "Induction of melanogenesis during the various melanoma growth phases and the role of tyrosinase, lysosome-associated membrane proteins, and p90 calnexin in the melanogenesis cascade," *Journal of Investigative*

Dermatology Symposium Proceedings, vol. 1, no. 2, pp. 195–202, 1996.

[8] E. Carrillo, J. Prados, J. A. Marchal et al., "Prognostic value of RT-PCR tyrosinase detection in peripheral blood of melanoma patients," *Disease Markers*, vol. 22, no. 3, pp. 175–181, 2006.

[9] C. Mangas, J. M. Hilari, C. Paradelo et al., "Prognostic significance of molecular staging study of sentinel lymph nodes by reverse transcriptase-polymerase chain reaction for tyrosinase in melanoma patients," *Annals of Surgical Oncology*, vol. 13, no. 7, pp. 910–918, 2006.

[10] Y. Tomita, "Tyrosinase gene mutations causing oculocutaneous albinisms," *Journal of Investigative Dermatology*, vol. 100, supplement 2, pp. 186S–190S, 1993.

[11] W. S. Oetting, "The tyrosinase gene and oculocutaneous albinism type 1 (OCA1): a model for understanding the molecular biology of melanin formation," *Pigment Cell Research*, vol. 13, no. 5, pp. 320–325, 2000.

[12] T. Suzuki and Y. Tomita, "Recent advances in genetic analyses of oculocutaneous albinism types 2 and 4," *Journal of Dermatological Science*, vol. 51, no. 1, pp. 1–9, 2008.

[13] M. Criton and V. Le Mellay-Hamon, "Dimeric cinnamoylamide derivatives as inhibitors of melanogenesis," *Biological and Pharmaceutical Bulletin*, vol. 34, no. 3, pp. 420–425, 2011.

[14] H. M. Wang, C. Y. Chen, and Z. H. Wen, "Identifying melanogenesis inhibitors from cinnamomum subavenium with in vitro and in vivo screening systems by targeting the human tyrosinase," *Experimental Dermatology*, vol. 20, no. 3, pp. 242–248, 2011.

[15] H. Ando, M. S. Matsui, and M. Ichihashi, "Quasi-drugs developed in Japan for the prevention or treatment of hyperpigmentary disorders," *International Journal of Molecular Sciences*, vol. 11, no. 6, pp. 2566–2575, 2010.

[16] H. Decker and F. Tuczek, "Tyrosinase/catecholoxidase activity of hemocyanins: structural basis and molecular mechanism," *Trends in Biochemical Sciences*, vol. 25, no. 8, pp. 392–397, 2000.

[17] L. Gou, Z. R. Lü, D. Park et al., "The effect of histidine residue modification on tyrosinase activity and conformation: inhibition kinetics and computational prediction," *Journal of Biomolecular Structure and Dynamics*, vol. 26, no. 3, pp. 395–402, 2008.

[18] Z. R. Lü, L. Shi, J. Wang et al., "The effect of trifluoroethanol on tyrosinase activity and conformation: inhibition kinetics and computational simulations," *Applied Biochemistry and Biotechnology*, vol. 160, no. 7, pp. 1896–1908, 2010.

[19] M. Shiino, Y. Watanabe, and K. Umezawa, "Synthesis and tyrosinase inhibitory activity of novel N-hydroxybenzyl-N-nitrosohydroxylamines," *Bioorganic Chemistry*, vol. 31, no. 2, pp. 129–135, 2003.

[20] D. Kim, J. Park, J. Kim et al., "Flavonoids as mushroom tyrosinase inhibitors: a fluorescence quenching study," *Journal of Agricultural and Food Chemistry*, vol. 54, no. 3, pp. 935–941, 2006.

[21] S. R. Kanade, V. L. Suhas, N. Chandra, and L. R. Gowda, "Functional interaction of diphenols with polyphenol oxidase. Molecular determinants of substrate/inhibitor specificity," *FEBS Journal*, vol. 274, no. 16, pp. 4177–4187, 2007.

[22] Q. Yan, R. Cao, W. Yi et al., "Synthesis and evaluation of 5-benzylidene(thio)barbiturate-β-D-glycosides as mushroom tyrosinase inhibitors," *Bioorganic and Medicinal Chemistry Letters*, vol. 19, no. 15, pp. 4055–4058, 2009.

[23] Y. D. Park, S. Y. Kim, Y. J. Lyou, J. Y. Lee, and J. M. Yang, "A new type of uncompetitive inhibition of tyrosinase induced by Cl-binding," *Biochimie*, vol. 87, no. 11, pp. 931–937, 2005.

[24] H. Y. Han, J. R. Lee, W. A. Xu, M. J. Hahn, J. M. Yang, and Y. D. Park, "Effect of Cl^- on tyrosinase: complex inhibition kinetics and biochemical implication," *Journal of Biomolecular Structure and Dynamics*, vol. 25, no. 2, pp. 165–171, 2007.

[25] M. X. Xie, X. Y. Xu, and Y. D. Wang, "Interaction between hesperetin and human serum albumin revealed by spectroscopic methods," *Biochimica et Biophysica Acta*, vol. 1724, no. 1–2, pp. 215–224, 2005.

[26] K. Arnold, L. Bordoli, J. Kopp, and T. Schwede, "The SWISS-MODEL workspace: a web-based environment for protein structure homology modelling," *Bioinformatics*, vol. 22, no. 2, pp. 195–201, 2006.

[27] G. M. Morris, R. Huey, W. Lindstrom et al., "AutoDock4 and AutoDockTools4: Automated docking with selective receptor flexibility," *Journal of Computational Chemistry*, vol. 30, no. 16, pp. 2785–2791, 2009.

[28] R. Huey, G. M. Morris, A. J. Olson, and D. S. Goodsell, "A semiempirical free energy force field with charge-based desolvation," *Journal of Computational Chemistry*, vol. 28, no. 6, pp. 1145–1152, 2007.

[29] J. L. Muñoz-Muñoz, F. Garcia-Molina, R. Varon et al., "Suicide inactivation of the diphenolase and monophenolase activities of tyrosinase," *IUBMB Life*, vol. 62, no. 7, pp. 539–547, 2010.

[30] Y. X. Si, S. J. Yin, D. Park et al., "Tyrosinase inhibition by isophthalic acid: kinetics and computational simulation," *International Journal of Biological Macromolecules*, vol. 48, no. 4, pp. 700–704, 2011.

[31] S. Khatib, O. Nerya, R. Musa, M. Shmuel, S. Tamir, and J. Vaya, "Chalcones as potent tyrosinase inhibitors: the importance of a 2,4-substituted resorcinol moiety," *Bioorganic and Medicinal Chemistry*, vol. 13, no. 2, pp. 433–441, 2005.

[32] B. Gasowska, P. Kafarski, and H. Wojtasek, "Interaction of mushroom tyrosinase with aromatic amines, o-diamines and o-aminophenols," *Biochimica et Biophysica Acta*, vol. 1673, no. 3, pp. 170–177, 2004.

[33] Y. D. Park, S. Y. Kim, Y. J. Lyou, D. Y. Lee, and J. M. Yang, "TXM13 human melanoma cells: a novel source for the inhibition kinetics of human tyrosinase and for screening whitening agents," *Biochemistry and Cell Biology*, vol. 84, no. 1, pp. 112–116, 2006.

[34] Y. D. Park, Y. J. Lyou, H. S. Hahn, M. J. Hahn, and J. M. Yang, "Complex inhibition of tyrosinase by thiol-composed Cu2+ chelators: a clue for designing whitening agents," *Journal of Biomolecular Structure and Dynamics*, vol. 24, no. 2, pp. 131–138, 2006.